Syngas production by chemical-looping gasification of waste activated carbon with iron-based oxygen carrier

Xiao Li
Qingdao University of Science and Technology
Mei An
Qingdao University of Science and Technology
Man Wu
Qingdao University of Science and Technology
Jinshuai Li
Qingdao University of Science and Technology
Xiuli Zhang
Qingdao University of Science and Technology
Jilai Wu
Qingdao University of Science and Technology
Sijie Yuan
Qingdao University of Science and Technology
Qingjie Guo (ajeedit01@126.com)
Qingdao University of Science and Technology

Research

Keywords: chemical looping gasification, cyclic properties, iron-based oxygen carrier, synthesis gas, waste activated carbon

Posted Date: May 7th, 2020

DOI: https://doi.org/10.21203/rs.3.rs-25900/v1

Abstract

Waste activated carbon (WAC), as a typical solid waste, can be utilized by chemical looping gasification (CLG) technology with an iron-based oxygen carrier to produce valuable synthesis gas products. A series of experiments on WAC of the CLG process were carried out in a fixed-bed reactor. The operation parameters involving the OC/WAC mole ratio, steam flow rate and reaction temperature during WAC CLG reactions were investigated in detail. Further, the cyclic performance within 10 cycles was also discussed. Fresh and other representative oxygen carrier samples were analyzed by X-ray diffraction (XRD) and scanning electron microscopy (SEM) characterization methods. The results showed that the optimal OC/WAC mole ratio, steam flow rate and reaction temperature were determined to be 0.15, 0.10 mL/min, and 950 °C, respectively, to obtain high-quality syngas with relatively high carbon conversion. The iron-based oxygen carrier exhibited a stable cyclic performance during the multiple tests, following the reaction path of $Fe_2O_3 \rightarrow Fe_{0.98}O$ in the individual reduction process. Moreover, the iron-based oxygen carrier could be oxidized almost to its initial state after 10 redox tests, and no obvious sintering and agglomeration phenomena were observed. The WAC of CLG presents a new approach for the comprehensive utilization and disposal of solid waste, especially with low volatile feedstocks.

1 Introduction

As the best versatile absorbent, activated carbon (AC) is extensively used in various industrial processes for decades, such as in pharmaceutical factories, sugar industry, and many other industries (Leong et al. 2018; Gamal et al. 2018). Because of the serious pore blockage, some of the spent activated carbon is difficult to either regenerate or reutilize. Thus, it is usually discarded as solid waste from factories. Furthermore, these discarded waste activated carbons (WACs) are commonly disposed for landfills and via open burning without treatment. Moreover, these disposal practices jeopardize the land security and threaten the air safety (Wong et al. 2018). Recognizing the aforementioned issues and considering the various disposal methods, the gasification technologies have attracted attentions due to their ability to convert carbonaceous waste to valuable products(Arnold and Hill 2019). However, the conventional gasification process has many drawbacks such as a demand for pure oxygen, external heat supplementation and high tar content than other methods. In addition, the oxygen source is expensive due to the requirement of the air separation unit (Shen et al. 2018). In order to overcome these problems, it is important to find more strategic methods for utilizing the nonrenewable WACs in a sustainable way. Typically, WAC has the advantages of high carbon content and a lack of a complex pretreatment, making it an acceptable candidate for use as a feedstock for gasification processes.

Against this background, chemical looping gasification is emerging as an innovative gasification technology (Wang et al. 2019), and has recently attracted considerable interest (Adanez et al. 2012; Wang et al. 2018). It derives from the concept of chemical looping combustion (CLC), which is associated with the inherent separation of CO_2 (Lyngfelt 2014), and it could convert carbon-containing feedstocks into value-added gas products in an oxygen-controlled atmosphere. Indeed, CLG is achieved with metal oxides (Me_xO_y) called oxygen carriers (OCs), which are employed as oxygen sources. The oxygen carrier is

continuously transported and circulated between two interconnected chambers. The oxygen required for gasification is provided by lattice oxygen released from the OC, which allows for a lower cost without air separation. Moreover, the lattice oxygen is capable of avoiding combustion reactions by controlling the mole ratio between fuels and OCs. The schematic diagram of CLG process for synthesis gas production was exhibited in Fig. 1.

The OC is the crucial backbone in the chemical looping process. Recently, a large number of oxygen carriers have been reported in CLG processes, such as Fe (Huang et al. 2016), Ni (Medrano et al. 2015), and Mn (Yin et al. 2018). These studies confirmed that the OCs are adoptable and feasible for the gasification of various carbon-containing fuels to produce synthesis gas products. Therefore, selecting the appropriate OC is significant. Apromising OC must be inexpensive, durable, stable, moderately reactive, nonpoisonous, and resistant to sintering or attrition (Zhao et al. 2017; Liu et al. 2018). All these needs make the iron-based OC the most common option. As it is able to meet the demand for efficient conversion within different feedstocks in chemical looping gasification (Huang et al. 2015; Liu et al. 2017). Huseyin et al. (2014) tested biomass CLG using Fe_2O_3/Al_2O_3 as an oxygen carrier in a 10 kWth interconnected fluidized bed reactor. The OC performed with good stability and reactivity during 60-h continuous runs. In particular, the Fe_2O_3/Al_2O_3 demonstrated excellent performance in the utilization of waste resources, such as sewage sludge, waste water and municipal solid waste (Chen et al. 2019). Huang et al. (2017)used natural hematite as an oxygen carrier in sewage sludge disposal. The results showed that the carbon conversion of fuel had increased by 36.29%, and the hematite also exhibited good performance during continuous tests for 23 h. Qin et al. (2018) investigated Fe_2O_3/Al_2O_3 using the CLR process of organic wastewater to produce high H_2/CO ratio syngas, and the results showed that almost 100% carbon conversion could be achieved; in addition, the highest syngas yield of 3.325 L/g was obtained, and Fe_2O_3/Al_2O_3 showed a notable performance and achieved auto-thermal feasibility in this CLR process.

Nevertheless, only a limited amount of studies on WAC disposal and treatment have been reported. The resource utilization and comprehensive use of WAC to produce synthesis gas were achieved by CLG, and this process opened a broader means for treatment of carbonaceous solid wastes and enabled a new application direction for its use in CLG. The purpose of this work is to verify the feasibility of using iron-based OCs for the use of WAC in CLG, focusing on macroscopic research combining various analytical methods. It is essential to determine suitable operation parameters, such as temperature, addition amount of OC, and gasifying agent, which are closely associated with the target gas quality, gasification performance and conversion rate (Weiland et al. 2015). Herein, a series of experiments were carried out to investigating the effect of some important parameters including the mole ratio between the OC and WAC, reaction temperature and steam flow on the gasification process. Afterward, the stability of the OC during multiple redox reactions was also discussed, and 10-cycle experiments were conducted. Finally, the fresh and used OC after its reaction with WAC were collected and analyzed with X-ray diffraction (XRD) and scanning electron microscopy (SEM) to better reveal the crystalline phase transformation and surface morphology changes, respectively.

2 Materials And Experimental

2.1 Materials

A typical waste activated carbon was collected from sugar factory waste in Shandong Province, China. Prior to testing, the samples were dried at 90 °C for 2 h and then ground and sieved into an approximate size of 80 ~ 200 μm. The proximate and ultimate analyses, and lower heating values of the WAC are provided in Table 1.

Table 1 Proximate and ultimate analysis of WAC after pretreatment

Sample	Proximate analysis w_{ad} (%)				Ultimate analysis w_{ad} (%)					LHV(MJ/kg)
	A	M	V	FC	C	H	N	S	O[]	
WAC	11.87	1.40	37.43	55.14	71.62	2.96	3.83	1.64	3.84	14.14

ad: air dried basis

[]: Calculatedby difference

2.2 Oxygen carrier preparation

The Fe_2O_3/Al_2O_3 oxygen carrier was prepared using the impregnation method. A given amount of $Fe(NO_3)_3.9H_2O$ was weighed as the active component and was dissolved in deionized water for preparation of the saturated solution. Here, Al_2O_3 powder was added into the saturated solution as an inert support, and the mixture solution was stirred and heated at 80 °C until the water was evaporated. After that, the residue was dried at 120 °C for approximately 12 h, after which it was transferred into a muffle furnace and calcined at 900 °C for approximately 3 h under an air atmosphere. Finally, the obtained precursors were crushed and sieved into ~ 100 μm to be ready for testing.

2.3 Experimental procedure

To simplify the CLG reaction process of WACs, a series of experiments were implemented in a fixed-bed reactor to test the feasibility of WAC disposal using CLG. The schematic diagram is illustrated in Fig. 2, and the details are briefly described as follows. The proposed apparatus is composed of a quartz tube reactor, a mass flow controller, a steam generator section, a cooling system, an exhaust gas sampling container, and an analysis system. The tube reactor was heated by an electronic furnace, and the temperature was controlled by a thermocouple surrounding the tube. The steam generator is composed of a constant flow pump for steam generation through preheating by a furnace at 300 °C, and the steam is sequentially introduced to the reactor.

In the reduction stage of each test, a mixture of WAC and oxygen carrier with various OC/WAC ratios (0, 0.1, 0.15, 0.2, and 0.25) was initially loaded in a quartz boat and placed on the cool zone of the tube.

High-purity argon was used as the purge gas at 200 mL/min for 15 min in advance to remove the air. When the reactor reached the desired reaction temperature (750, 800, 850, 900, and 950 °C), argon was replaced by a mixture stream of different steam flow rates (0, 0.05, 0.10, 0.15, and 0.20 mL/min). Next, the argon was used to flush the gasification reactor for 5 min. After that, the quartz boat was rapidly moved into the heating zone, and the gasification time was 60 min, which was sufficient time for the reaction. The exit gas was passed through for cooling, purifying and drying, and the generated gases were collected via a group of sampling bags at 5 min intervals. During the oxidation period, the reduced OC was oxidized by air at a volumetric flow rate of 200 mL/min in a tubular furnace, and the oxidation time was set to 60 min. Since the reaction system was a batch system, the OC particles were alternatively exposed to oxidation and reduction stages to simulate the circulating experiments. The compositions of the flue gas were measured by off-line gas chromatography with high-purity argon (99.995%) as the carrier gas with a TCD detector. After the reactor cooled to ambient temperature, the selected oxygen carrier particles were collected for characterization analysis.

2.4 Oxygen carrier Characterization

To better understand the reaction mechanism, a series of characterization methods were employed. The crystalline phase of the oxygen carrier samples before and after reduction and of the samples after multi-cycle tests were confirmed with X-ray diffraction using Cu-Kα radiation with 40 kV and a current of 40 mA. The samples were scanned in the 2θ range of 5–80 ° with a step range of 0.02 °. Moreover, scanning electron microscopy (SEM) using a Hitachi S4800 was used to evaluate the morphology surface features of the oxygen carrier samples at the different stages.

2.5 Data processing

(1) In each part, the relative gas content (C_i) of each component in the dry basis outlet gas can be evaluated as follows:

$$C_i = \frac{\int_0^t v \cdot y_i \, dt}{\int_0^t v \cdot y \, dt} \quad (1)$$

where y_i represents the actual volume fraction of gas species i (H_2, CO, CH_4, and CO_2) in the dry outlet gas and parameter v denotes the volume flow rate of the dry basis flue gas in the outlet.

(2) The lower heating value (LHV, MJ/Nm^3) of the generated gas products can be calculated as follows:

$$LHV = 126 C_{CO} + 108 C_{H2} + 388 C_{CH4} \quad (2)$$

(3) The gas yield (G_v, Nm^3/kg) is the volume of dry basis gas product yielded from the unit mass of WAC sample, calculated as follows:

$$G_v = \frac{\int_0^t v \cdot (y_{CO} + y_{CO2} + y_{CH4} + y_{H2}) dt}{M_{WAC}} \quad (3)$$

(4) The carbon conversion efficiency of the WAC (η_c,%) is revealed as follows, which is the proportion of the carbon fraction of carbon-containing gas in the outlet gas to the carbon fraction of the WAC fed into reactor, where C_C % is the carbon content of the WAC:

$$\eta_c=\frac{12(C_{co}+C_{co_2}+C_{CH_4})\cdot G_v}{24.45\cdot Cc\%\cdot M_{WAC}} \quad (4)$$

(5) The effective gas content (Y_g, %) is defined as the ratio of the volume of effective gases (H_2, CO, CH_4) to the total amount of gas produced by WAC:

$$Y_g=\frac{\int_0^t(V_{CO}+V_{H_2}+V_{CH_4})dt}{\int_0^t(V_{CO}+V_{CO_2}+V_{CH_4}+V_{H_2})dt} \quad (5)$$

(6) The syngas yield (Nm^3/kg) is the addition of effective gas yield:

$$V_g=\frac{\int_0^t v\cdot(y_{CO}+y_{CO_2}+y_{CH_4})dt}{M_{WAC}} \quad (6)$$

Active composition Fe_2O_3contained in iron-based OC is just considered to reduce to Fe_3O_4.

3 Results And Discussion

3.1 Effect of (OC/WAC) ratio

The OC is displayed as an oxygen source and heat carrier, and it causes a positive effect on fuel conversion during CLG process. Thus, a series of comparison experiments were conducted to obtain the optimal OC/WAC value. In addition, Al_2O_3 had no active role, and it was used as the bed material for the blank experiment for comparison.

The effect of OC/WAC mole ratio on gas distribution and LHV were shown in Fig. 3a. H_2 was consumed at first, by the reaction (7) due to the low activation energy. Thus H_2 content gradually decreased with the increase of OC/WAC. Mainly ascribed to the supplement of suitable lattice oxygen put rightward the reaction (10), CO concentration firstly increased when OC/WAC lower than 0.1. However, COdeclined sharply while the CO_2 inclined monotonously as the OC/WAC increased from 0.10 to 0.25. This can be explained that excess lattice oxygen promoted the reactions shown in reaction (7) and (8), and consumed combustible gases to more CO_2 and H_2O generation, indicating that gasification process gradually replaced by combustion process in this case.CH_4 content declined slightly with an increasing OC/WAC, on account of the reaction (9). Meanwhile, LHV firstly increased improved at the OC/WAC range of 0 to 0.1, reaching its maximal of 7.70 MJ/Nm^3. And then abruptly decreased when OC/WAC exceeded 0.10, and its minimum value of 5.66 MJ/Nm^3 was obtained at OC/WAC of 0.25. The results attributed to extra OC provided excess lattice oxygen, causing the consumption of large amount synthesis gas.

In order to further understand the effect of OC on CLG process of treating WAC, the vital variables of carbon conversion, syngas concentration and syngas yield were shown in Fig. 3b. Due to the more OC obviously promoting the WAC conversion, carbon conversion gradually increased from 32.72–75.53% as the increasing of OC/WAC from 0 to 0.25. Moreover, syngas concentration and syngas yield were up to 67.41% and 1.12 Nm^3/kg, respectively. It resulted that syngas generation were evidently enhanced when in the presence of OC addition. A proper addition amount of OC is prone to achieve the partial oxidize the WAC, producing the target gaseous products (Wei et al. 2019). Additionally, the OC inventory enhances water-gas shift reaction equilibrium toward products direction to generate more H_2 (Deng et al. 2019). However, when in the cases that OC/WAC was bigger than 0.1, syngas concentration drastically decreased, and syngas yield gradually decreased as well. This mainly attributed to a part of combustible gas was completely oxidized within excess lattice oxygen provided by excess OC. It is adverse to syngas generation. In general, relatively high OC/WAC meant more OC added in reactor, which significantly promoted WAC conversion but sacrificed synthesis gas yield. Aiming at the target of high-efficiency resource utilization and disposal of WAC, the OC/WAC ratio was determined at 0.15, where ensured the disposal principle of higher WAC conversion avoiding the complete oxidation the gaseous products with the highest LHV value of 7.67 MJ/$Nm^3$was obtained. The reactions associated with OC are listed as followed:

$H_2 + 1.042Fe_2O_3 = 2.127Fe_{0.98}O + H_2O \ \triangle H_{1173K} > 0 \ \triangle G_{1173K} < 0$ (7)

$CO + 1.042Fe_2O_3 = 2.127Fe_{0.98}O + CO_2 \ \triangle H_{1173K} < 0 \triangle G_{1173K} < 0$ (8)

$CH_4 + 4.17\ Fe_2O_3 = 8.511Fe_{0.98}O + CO_2 + 2H_2O \ \triangle H_{1173K} > 0 \triangle G_{1173K} < 0$ (9)

$C + 1.042Fe_2O_3 = 2.127Fe_{0.98}O + CO \ \triangle H_{1173K} > 0 \triangle G_{1173K} < 0$ (10)

3.2 Effect of steam flow rate

Considering the target of further enhancing the WAC conversion and synthesis gas yield, especially the H_2 yield, steam was employed as a gasifying agent during the CLG of WACs. In this study, the effect of steam addition on syngas yield was studied.

The flue gas concentration and LHV variation under different steam flow rates are shown in Fig. 4a. In the absence of steam, it can be seen that the H_2 concentration was the lowest at 17.69%, but CO_2 was the highest at 65.07%, and the LHV attained its minimum value of 4.18 MJ/Nm^3 in this case as well. With the increase in steam flow rate, the H_2 concentration showed an evident uptrend, whereas the CO concentration decreased overall. This can be interpreted as more reactants facilitating a shift in the water-gas shift reaction (12) and causing the equilibrium to shift toward the right to more H_2 generation and CO consumption. It is noteworthy that the CO content presented a fluctuation trend, possibly because of the competition effects between reactions (11), (12) and (13). The CO_2 concentration decreased overall, and it was much lower than that of the experiments without steam. Because the WACs have high fixed carbon content, they preferentially react with steam to generate CO rather than undergoing solid-

solid reactions between OC and WAC particles. For CH_4, its concentration remained nearly invariable. Based on evaluations of the synthesis gas concentration, the LHV increased substantially from 4.18 MJ/Nm^3 to 6.95 MJ/Nm^3 as the steam flow rate reached 0.05 mL/min, but the LHV increased mildly when the flow rate was greater than 0.10 mL/min. This result suggests that an appropriate steam addition significantly improves the syngas yield, especially H_2 generation, which contributes to enhanced quality of the synthesis gas.

$C + CO_2 = 2CO \ \triangle H_{1173K} = +168.84$ kJ/mol (11)

$C + H_2O = CO + H_2 \ \triangle H_{1173K} = +135.71$ kJ/mol (12)

$C + 2H_2O = CO_2 + H_2 \ \triangle H_{1173K} = +141.3$ kJ/mol (13)

$CO + H_2O = CO_2 + H_2 \ \triangle H_{1173K} = -41.18$ kJ/mol (14)

Additionally, the effect of steam flow rate on carbon conversion, syngas concentration and syngas yield is displayed in Fig. 4b. Carbon conversion presented an increasing tendency as the steam flow rate reached 0.10 mL/min and reached a maximum value of 60.3% at 0.10 mL/min. While the flow rate was more than 0.10 mL/min, carbon conversion decreased slightly with the continuous increase in steam flow rate. The syngas concentration first decreased and then gradually increased to 66.9% at 0.20 mL/min. The syngas yield presented an overall uptrend; after first growing rapidly, the yield growth became moderate, which may have resulted from the reduction reactions being close to chemical equilibrium. On the one hand, steam acted as an oxygen source integrated with a single oxygen source supplied by the OC, which could evidently promote carbon conversion and improve the contact between solid reactants. Accordingly, solid-solid reactions between the OC and solid reactant particles were improved (Huang et al. 2016). On the other hand, more reactants promoted a shift toward reaction equilibrium, and more steam facilitated the water-gas shift reaction to the right to generate more H_2. Generally, the steam introduction actually accelerates the syngas yield, especially H_2 yield. However, it is notable that excessive steam (> 0.10 mL/min) had no apparent impact on carbon conversion except for increasing the cost. At the same time, more steam addition would shorten the residence time between the gas phase and solid phase, and the reactions between the WAC and steam were particularly inhibited; thus, the WAC conversion and gas yield were restricted within low steam amounts. The flow rate of 0.10 mL/min was selected as the proper steam flow rate, where the carbon conversion with syngas reached 60.3% and an acceptable LHV of 7.15 MJ/Nm^3 was achieved.

3.3 Effect of reaction temperature

Reaction temperature is a key parameter that closely influences the fuel conversion and OC performance in CLG (Taba et al. 2012). In this study, a series of experiments corresponding to the effect of gasification temperature on WAC CLG were implemented.

Furthermore, the effects of temperature on carbon conversion and syngas concentration are shown in Fig. 5b. As a result, a higher gasification temperature was conducive for not only WAC thermal conversion but also syngas yield. Accordingly, the syngas concentration presented a monotonically increasing trend with the ramping up of the temperature. The carbon conversion increased drastically from 26.59% to 71.54% as the temperature increased from 750 °C to 950 °C. Meanwhile, the syngas yield attained maximum values of 1.43 Nm^3/kg at 950 °C. It is well known that higher temperatures facilitate the exothermic reactions (10), (11) and (12), causing the chemical equilibrium to shift toward the right on the basis of Le Chatelier's principle, as shown in the WGS reaction and the Boudouard reaction. On the other hand, the high reaction temperature inhibited the endothermic reaction and consumed the CO_2. These results are mainly attributed to two aspects. One was that high temperature enhances the endothermic reactions, and the content of CO and H_2 increased with increasing temperature. In addition, the OC presented poor reactivity under lower temperatures, leading to carbon conversion, and the syngas products were limited. When the temperature reached 900 °C, more lattice oxygen was released andfurther enhanced the WAC conversion. Generally, a high reaction temperature is necessary for WAC thermal conversion and high-quality synthesis gas yields. Thus, 950 °C was the optimum reaction temperature for the CLG process of WAC, where all the important parameters of carbon conversion, syngas yield, and LHV attained maximum values of 71.54%, 1.47 Nm^3/kg, and 7.39 MJ/Nm^3, respectively.

3.4 Effect of numbers of cycles

Reactivity stabilization is the key issue for employing OCs as optimal candidates in the CLG process. Based on the aforementioned results, multi-cycle tests were carried out in a fixed-bed reactor to evaluate the cycle reactivity of the OCs in the CLG process. In each run, the reaction temperature, OC/WAC, steam flow rate, and reaction time were fixed at 900 °C, 0.15, 0.10 mL/min and 60 min, respectively.

As illustrated in Fig. 6a, the concentration of CO_2 showed a slight downward trend with the increase in cycle numbers, while the CO concentration presented a slight upward trend during all cycling tests. The concentration of H_2 also increased over the cycles and fluctuated at an acceptable range from 49.50% to 53.21%. There was no remarkable change in CH_4 content. Based on the above analysis of the gas distribution results, the value of LHV increased from 7.09 MJ/Nm^3 in the 1st redox cycle to 7.75 MJ/Nm^3 in the 10th cycle. It can be speculated that the OC reactivity showed a slight deactivation trend after 10 cycles, especially when the oxidation ability of the OC tended to be moderate, leading to a slight decrease in CO_2 concentration and an elevated calorific value of gases. Further, as shown in Fig. 6b, the carbon conversion first increased over the former redox cycles but then showed a downward trend from 58.95–53.11% during the whole tests. The syngas concentration gradually increased with the number of cycles and reached a maximum value of 65.28% in the 10th cycle. Meanwhile, the syngas yield slightly increased and remained above 1.03 Nm^3/kg. Although the reactivity of the OC showed a down ward trend after multiple cycles, the generated gases from the lowest carbon conversion of 53.11% and synthesis gas yield of 72.13% within 10 cycles were still much higher than those in the CLG of WAC in the absence

of OC, where the carbon conversion and syngas yield were 32.72% and 0.19 Nm^3/kg, respectively. Therefore, Fe_2O_3/Al_2O_3 presented a favorable cycle performance in a comparatively long run of cycles for the CLG of WAC, and the variation in the OC performance was analyzed with different characterization methods and is discussed in detail in the next section.

3.5 Characterization of OCs

To further understand the reactivity variation in OCs during the multi-cycle test, the crystalline phase transformation and surface morphology of the OCs were characterized by XRD and SEM. The fresh OC and the OC samples after the 1st reduction and the 10th redox cycle were collected for analysis.

The XRD patterns of samples in different stages of the WAC CLG process are shown in Fig. 7. The fresh OC mainly consisted of Fe_2O_3 and Al_2O_3. The Fe_2O_3 was the active component and oxygen carrier to release lattice oxygen, achieving partial oxidation and conversion of the WAC in the CLG process, and Al_2O_3 was displayed as an inert carrier. After the 1st reduction process of the OC in the CLG process of the WAC, the crystalline phases of $Fe_{0.98}O$ and Al_2O_3were detected. This indicated that $Fe_{0.98}O$ was the predominant crystal formed from the active component after the individual reduction. The active oxygen carrier component Fe_2O_3 was reduced to $Fe_{0.98}O$ after CLG of the WAC. Accordingly, on the basis of the crystalline phase transformation observed from XRD, the reduction process of Fe_2O_3/Al_2O_3 follows the path $Fe_2O_3 \rightarrow Fe_{0.98}O$. Negative changes to the particles including through sintering and agglomeration usually occurred during the phase transition from FeO to Fe (Adanez et al. 2012). Meanwhile, little change could be observed in the inert Al_2O_3 phase, although it has no ability to release lattice oxygen and directly reacts with the WAC at high temperature. Additionally, the unreacted fuel and WAC ash covered the OC surface, which is responsible for the reduction in the Al_2O_3 phase.

It can be observed in Fig. 7 that the main diffraction peaks of Fe_2O_3 (PDF: 33–0664) are the main active constituents and that Al_2O_3 (PDF: 04-0877) is the inert constituent in the 10th cycle sample, and this is similar to the fresh sample, implying that after multi-redox cycles, the iron-based OC has been almost regenerated to its original state over the oxidation stage. The iron-based oxygen carrier had a favorable cycle performance in the CLG process.

Scanning electron microscopy (SEM) was used to evaluate the morphology and shape of OC samples after undergoing different reaction stages. As illustrated in Fig. 8a, the surface structure of the fresh sample was tough and loose with a porous structure, which was beneficial for the diffusion and reactions of reactants (Das et al. 2018). After the 1st cycle, a greater porosity structure was observed than that of fresh sample, which was ascribed to gas escaping from the interior of the OC particles (Deng et al. 2019). In this case, the structure was conducive for the penetration of gaseous reactants into the core of the OC particles, which was responsible for the slight increase in performance in the former cycles. Finally, as shown in Fig. 8c, agglomeration was observed in the 10th sample, and some small granules merged into larger granules, which was adverse to the reaction between the OC and other reactants. This may have resulted from the lattice transfer and continuous thermal stress at high temperatures during the multiple

tests. Some WAC ash might block the pore and cause a negative change to the surface structure as well, but it still remained porous. In addition, the sufficient number of oxygen carriers could moderate the risk of the sintering phenomena. These results indicate that iron-based oxygen carriers are a promising candidate in the WAC CLG process.

4. Conclusions

This work focused on verifying the feasibility of WAC as a feedstock to CLG using an iron-based oxygen carrier to produce a syngas product. The iron-based oxygen carrier showed favorable reactivity for syngas generation and WAC conversion. The effects of some operation parameters have been examined on a bench-scale fixed-bed reactor. The following conclusions are drawn based upon the results:

(1) The optimal OC/WAC mole ratio was determined at 0.15, where the highest yield of syngas product of 1.12 Nm^3/kg and an acceptable carbon conversion of 60.31% were obtained based on the tradeoff between WAC conversion and syngas yield.

(2) An adequate amount of steam introduction would promote WAC conversion and hydrogen generation. Therefore, a relatively high carbon conversion of 60.31% and an LHV of 6.95 MJ/Nm^3 were reached at a suitable steam flow rate of 0.10 mL/min .

(3) When the reaction temperature was 950 °C, the carbon conversion, syngas yield and LHV were maximized.

(4) The cyclic performances of the OC during 10-time cycle tests were evaluated. No obvious change occurred in the crystalline phase and morphology structure over the long run, and the iron-based oxygen carrier exhibited good cycling performance based on the analysis results of XRD and SEM.

(5) The oxygen carrier followed the reaction path of $Fe_2O_3 \rightarrow Fe_{0.98}O$ in the individual reduction process, and then it could be oxidized to its initial state after 10 redox cycle tests. In general, comprehensive WAC disposal in a highly efficient and environmentally friendly way was achieved by the CLG process with an iron-based oxygen carrier.

Abbreviations

AC	Activated carbon
WAC	Waste activated carbon
CLC	Chemical looping combustion
CLG	Chemical looping gasification
Me_xO_y	Metal oxide

OC	Oxygen carrier
CLR	Chemical looping reforming
A	Ash (wt%)
M	Moisture(wt%)
V	Volatile (wt%)
FC	Fixed carbon (wt%)
TCD	Temperature controlled detector
M	The mass of WAC (g)
LHV	Lower heat value
XRD	X-ray diffraction
SEM	Scanning electron microscopy
WGS	Water gas shift

Declarations

Acknowledgments

This work is funded by the Key Research and Development Program Project the Ningxia Hui Autonomous region (2018BCE01002); The National Natural Science Foundation of China (201868025); The National Key Research and Development Program Project (2018YFB0605401); The National First-rate Discipline Construction Project of Ningxia (NXYLXK2017A04); The Key Research and Development Program Ningxia (2018BEE03009).

References

Adanez J, Abad A, Garcia-Labiano F, Gayan P, Diego L F D (2012) Progress in chemical-looping combustion and reforming technologies. Progress in Energy & Combustion Science 38(2): 215-282.

Arnold RA, Hill JM (2019) Catalysts for gasification: a review. Sustainable Energy & Fuels 181(3): 656-672.

Chen P, Sun X, Gao M, Ma J, Guo Q (2019) Transformation and migration of cadmium during chemical-looping combustion/gasification of municipal solid waste. Chemical Engineering Journal 365: 389-399.

Das S, Deen NG, Kuipers HAM (2018) Multi-scale modeling of fixed-bed reactors withporous (open-cell foam) non-spherical particles: Hydrodynamics. Chemical Engineering Journal 334:741-759.

Deng Z, Huang Z, He F, Zheng A, Wei G, Meng J, Zhao Z, Li H (2019) Evaluation of calcined copper slag as an oxygen carrier for chemical looping gasification of sewage sludge. International Journal of Hydrogen Energy 44(33): 17823-17834.

Gamal MEl, Mousa HA, El-Naas MH, Zacharia R, Judd S (2018) Bio-regeneration of activated carbon: a comprehensive review. Separation and Purification Technology 197: 345-359.

Huang Z, He F, Zhu H, Chen D, Zhao K, Wei G, Feng Y, Zheng A, Zhao Z, Li H (2015) Thermodynamic analysis and thermogravimetric investigation on chemical looping gasification of biomass char under different atmospheres with Fe_2O_3 oxygen carrier. Applied Energy 157: 546-553.

Huang Z, Xu G, Deng Z, Zhao K, He F, Chen D, Wei G, Zheng A, Zhao Z, Li H (2017) Investigation on Gasification Performance of Sewage Sludge Using Chemical Looping Gasification with Iron Ore Oxygen Carrier. International Journal of Hydrogen Energy 42(40): 25474-25491.

Huang Z, Zhang Y, Fu J, Yu L, Chen M, Liu S, He F, Chen D, Wei G, Zhao K, Zheng A, Zhao Z, Li H (2016) Chemical looping gasification of biomass char using iron ore as an oxygen carrier. International Journal of Hydrogen Energy 41(40): 17871-17883.

Huseyin S, Wei G, Li H, He F, Huang Z (2014) Chemical-looping gasification of biomass in a 10 kWth interconnected fluidized bed reactor using Fe_2O_3/Al_2O_3 oxygen carrier. Journal of Fuel Chemistry and Technology 42(8): 922-931.

Leong KY, Loo SL, Bashir MJK, Oh WD, Rao PV, Lim J (2018) Bio-regeneration of spent activated carbon: Review of key factors and recent mathematical models of kinetics. Chinese Journal of Chemical Engineering 23(5): 893-902.

Lyngfelt A. (2014) Chemical-looping combustion of solid fuels, Status of development. Applied Energy 113(1):1869-1873.

Medrano JA, Hamers HP, Williams G, Annaland MS, Gallucci F (2015) $NiO/CaAl_2O_4$ as active oxygen carrier for low temperature chemical looping applications. Applied Energy 158:86-96.

Liu GC, Liao YF, Wu Y. (2017) Characteristics of microalgae gasification through chemical looping in the presence of steam. International Journal of Hydrogen Energy 42(36): 22730-22742.

Liu GC, Liao YF, Wu Y, Ma X (2018) Application of calcium ferrites as oxygen carriers for microalgae chemical looping gasification. Energy Conversion & Management (160): 262-272.

Qin W, Wang J, Luo L, Liu L, Xiao X, Zheng Z, Sun S, Hu X, Dong C (2018) Chemical looping reforming of ethanol-containing organic wastewater for high ratio H_2/CO syngas with iron-based oxygen carrier,

International Journal of Hydrogen Energy 43(29): 12985-12998.

Shen T, Ge H, Shen L (2018) Characterization of combined Fe-Cu oxides as oxygen carrier in chemical looping gasification of biomass. International Journal of Greenhouse Gas Control 75: 63-73.

Taba LE, Irfan MF, Wan Daud WAM, Chakrabarti MH (2012) The effect of temperature onvarious parameters in coal, biomass and CO-gasification: a review. Renewable and Sustainable Energy Reviews 16(8): 5584-96.

Wang Y, Niu P, Zhao H (2019) Chemical looping gasification of coal using calcium ferrites as oxygen carrier. Fuel Processing Technology 192: 75-86.

Wang S, Yin W, Li Z, Yang X, Zhang K (2018) Numerical investigation of chemical looping gasification process using solid fuels for syngas production. Energy Conversion and Management 173: 296-302.

Weiland F, Wiinikka H, Hedman H, Wennebro J, Pettersson E, Gebart R (2015) Influence of process parameters on the performance of an oxygen blown entrained flow biomass gasifier. Fuel 153: 510-519.

Wei G, Wang H, Zhao W, Huang Z, Yi Q, He F , Zhao K, Zheng A, Meng J, Deng Z, Chen J, Zhao Z , Li H (2019) Synthesis gas production from chemical looping gasification of lignite by using hematite as oxygen carrier. Energy Conversion and Management 185: 774-782.

Wong S, Ngadi N, Inuwa IM, Hassan O (2018) Recent advances in applications of activated carbon from biowaste for wastewater treatment: A short review, Journal of Cleaner Production 175: 361-375.

Yin S, Shen L, Dosta M, Hartge EU, Heinrich S, Lu P, Werther J, Song T (2018) Chemical looping gasification of biomass pellet with a Manganese ore as oxygen carrier in the fluidized bed. Energy & Fuels 32 (11): 11674-11682.

Zhao X, Zhou H, Sikarwar VS, Zhao M, Park AHA, Fennell PS, Shen L, Fan LS (2017) Biomass-based chemical looping technologies: the good, the bad and the future. Energy & Environmental Science, 10 (9): 1885-1910.

Figures

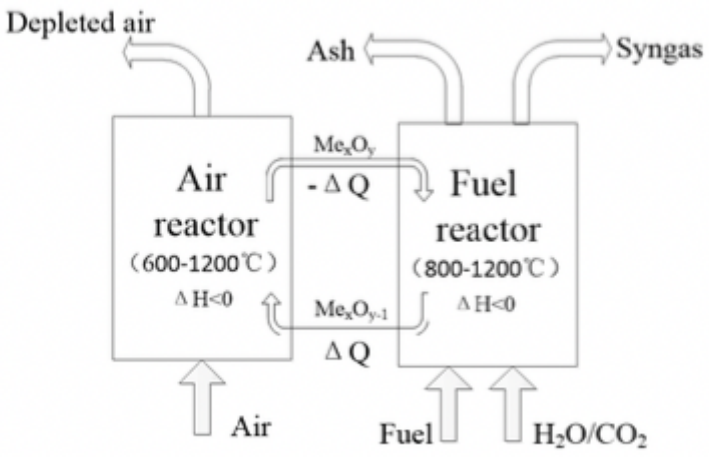

Figure 1

Schematic of a fixed bed reactor.

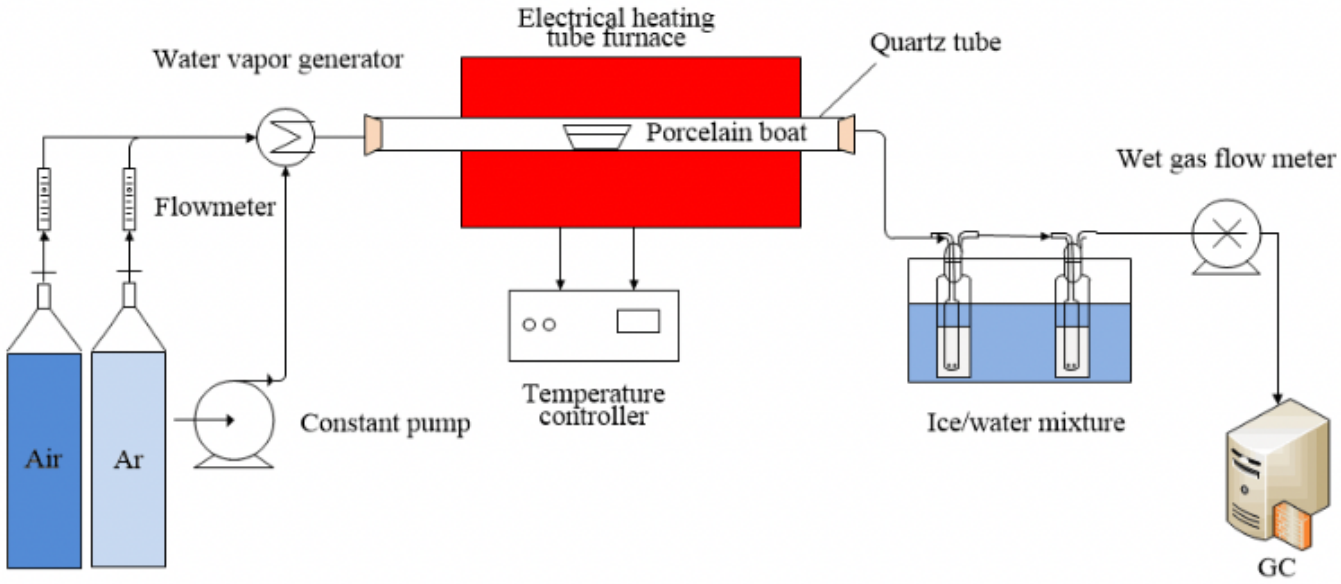

Figure 2

Schematic of a fixed bed reactor

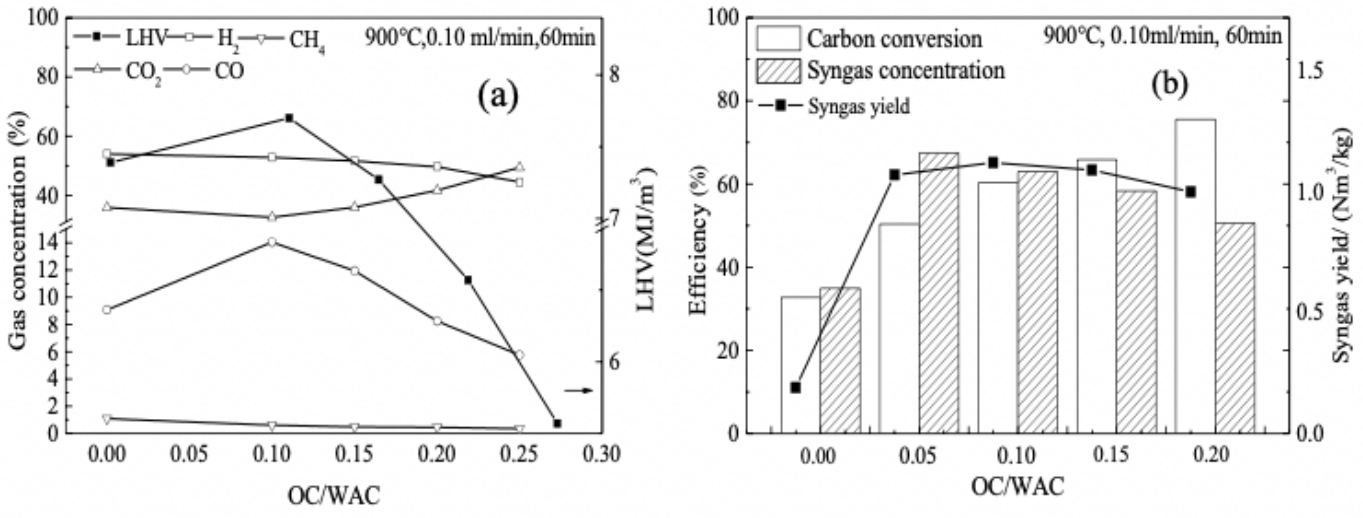

Figure 3

Gasification characteristics of WAC with different OC/WAC

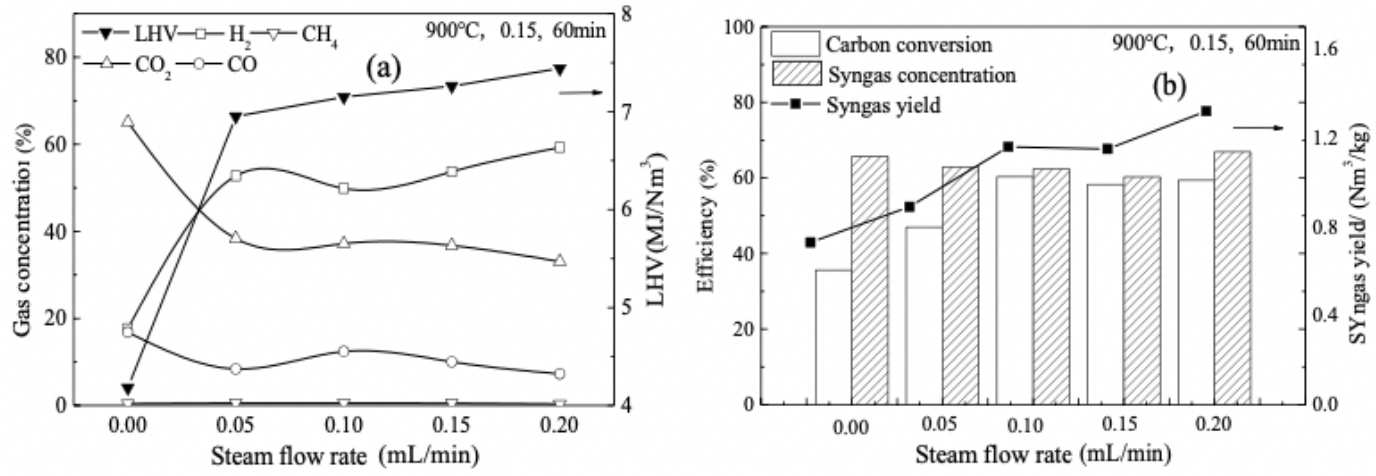

Figure 4

Gasification characteristics of WAC with different steam flow rate

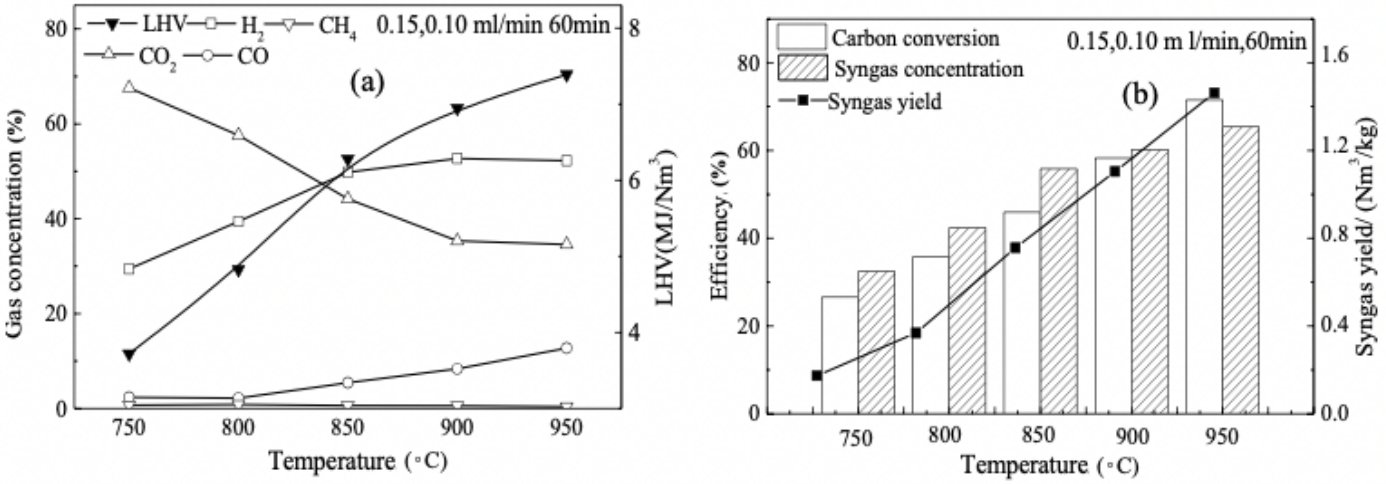

Figure 5

Gasification characteristics of WAC under different temperature

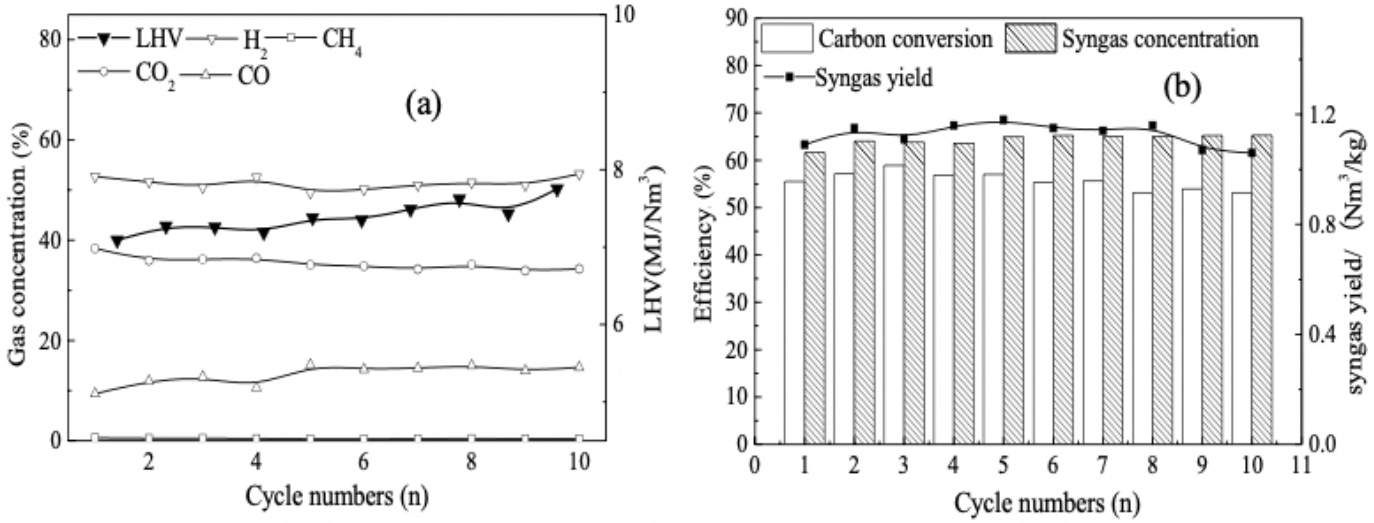

Figure 6

Gasification characteristics of WAC under different temperature

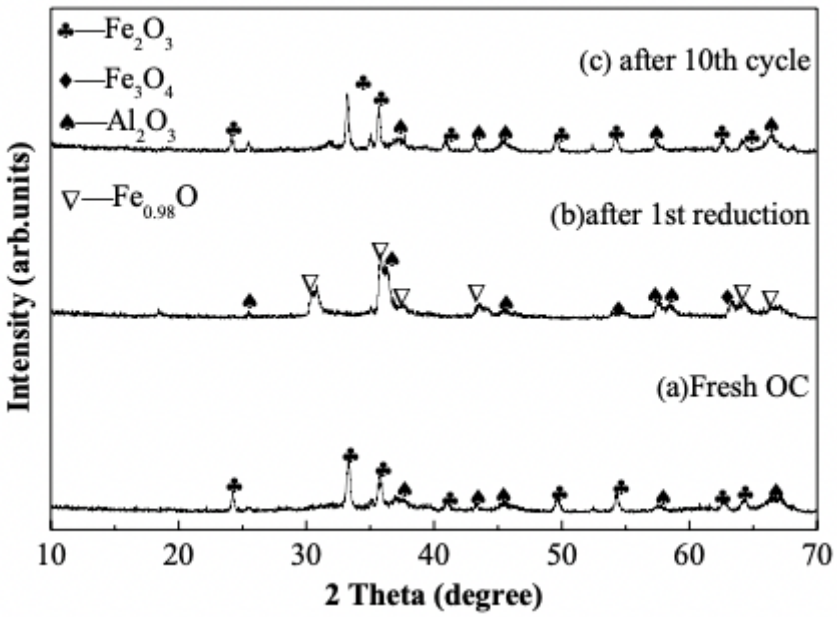

Figure 7

XRD patterns of fresh and used OC samples

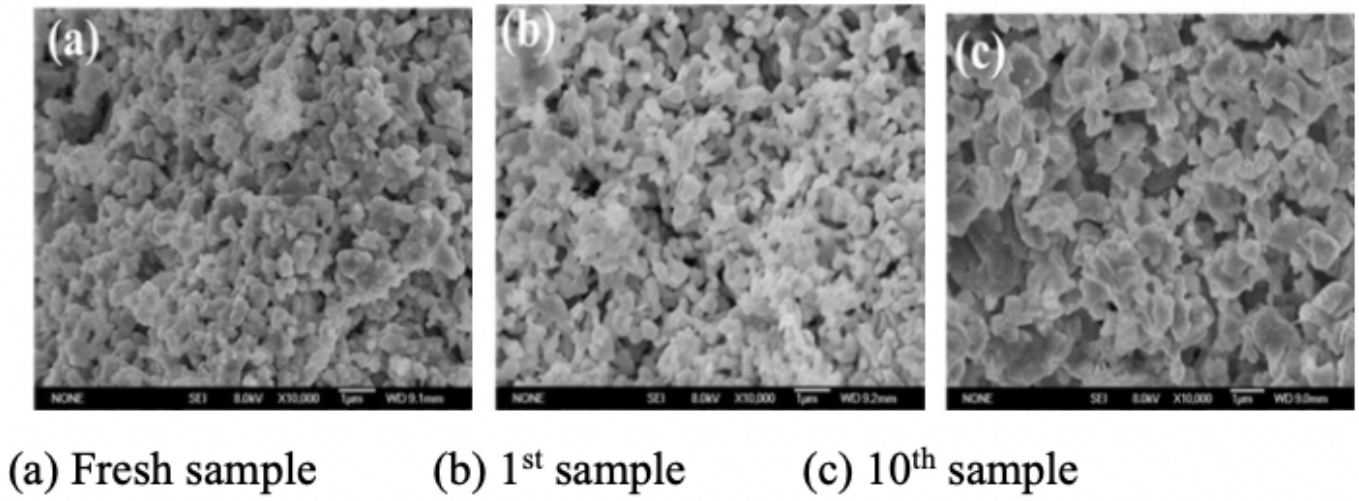

Figure 8

SEM images of Fresh and used OC samples